Data-Driven Scheduling of Energy Storage in Day-Ahead Energy and Reserve Markets with Probabilistic Guarantees on Real-Time Delivery

Jean-François Toubeau, *Member, IEEE,* Jérémie Bottieau, *Student Member, IEEE,*
Zacharie De Grève, *Member, IEEE,* François Vallée, *Member, IEEE* and Kenneth Bruninx, *Member, IEEE*

***Abstract*—Energy storage systems (ESS) may provide the required flexibility to cost-effectively integrate weather-dependent renewable generation, in particular by offering operating reserves. However, since the real-time deployment of these services is uncertain, ensuring their availability requires merchant ESS to fully reserve the associated energy capacity in their day-ahead schedule. To improve such conservative policies, we propose a data-driven probabilistic characterization of the real-time balancing stage to inform the day-ahead scheduling problem of an ESS owner. This distributional information is used to enforce a tailored probabilistic guarantee on the availability of the scheduled reserve capacity via chance constrained programming, which allows a profit-maximizing participation in energy, reserve and balancing markets. The merit order-based competition with rival resources in reserve capacity and balancing markets is captured via a bi-level model, which is reformulated as a computationally efficient mixed-integer linear problem. Results show that a merchant ESS owner may leverage the competition effect to avoid violations of its energy capacity limits, and that the proposed risk-aware method allows sourcing more reserve capacity, and thus more value, from storage, without jeopardizing the real-time reliability of the power system.**

***Index Terms*—Chance-constrained programming, Data-driven optimization, Energy storage, Energy-operating reserve markets, Balancing markets.**

NOMENCLATURE

A. Superscripts

ch	Charge mode of storage system.
d	Downward reserve.
da	Downward reserve activation.
dis	Discharge mode of storage system.
u	Upward reserve.
ua	Upward reserve activation.

B. Sets and indices

$\mathcal{G}$	Set of G conventional generators, index g.
$\mathcal{J}$	Set of J demands, index j.
$\mathcal{L}$	Set of L reserve activation levels, index l.
$\mathcal{T}$	Set of T time steps, index t.
$\mathcal{W}$	Set of W renewable generators, index w.

C. Upper-level decision variables

e_t	Stored energy in the ESS at time t, MWh.
$\hat{o}_t$	Price bid/offer at time t, €/MWh.
$\hat{p}_t$	Offered quantity in the energy market at time t, MWh/h.
$\hat{u}_t, \hat{d}_t$	Offered upward and downward reserve capacity in day-ahead at time t, MW.

D. Lower-level decision variables and dual variables

p_t	Scheduled quantity in the day-ahead energy market at time step t, MWh/h.
u_t, d_t	Allocated upward and downward reserve capacity at time step t, MW.
$ua_{l,t}, da_{l,t}$	Activated upward and downward reserve in level l at time step t, MWh.
λ_t^{e}	Electricity price in the day-ahead market at time step t, €/MWh.
$\lambda_t^{\mathrm{u}}, \lambda_t^{\mathrm{d}}$	Upward (u) and downward (d) reserve capacity price at time step t, €/MW.
$\lambda_{l,t}^{\mathrm{ua}}, \lambda_{l,t}^{\mathrm{da}}$	Upward (ua) and downward (da) reserve activation or balancing price at time step t in level l, €/MWh.

E. Parameters

$A_l^{\mathrm{u}}, A_l^{\mathrm{d}}$	Upward (u) and downward (d) reserve activation volume in level l, MW.
$C^{\mathrm{ch}}, C^{\mathrm{dis}}$	Operating costs of ESS in charge (ch) and discharge (dis) modes, €/MWh.
C_g, C_j	Marginal cost of generation g, and utility of demand j €/MWh.
$D_{j,t}$	Maximum load of demand j at time t, MW.
$\underline{E}, \overline{E}$	Lower and upper energy bounds of ESS, MWh.
E^{target}	End of day target state-of-charge of ESS, MWh.
$\eta^{\mathrm{ch}}, \eta^{\mathrm{dis}}$	ESS charge (ch) and discharge (dis) efficiency.
$\overline{P}^{\mathrm{ch}}, \overline{P}^{\mathrm{dis}}$	Maximum power of ESS in charge (ch) and discharge (dis) modes, MW.
$\overline{P}_g$	Maximum power capacity of generator g, MW.
$P_{l,t}^{\mathrm{u}}, P_{l,t}^{\mathrm{d}}$	Probability of reaching upward (u) and downward (d) reserve activation level l at time step t.
$\overline{P}_{w,t}$	Wind power forecast of producer w at time t, MW.

The work is supported via the energy transition funds project 'EPOC 2030-2050' organized by the FPS economy, S.M.E.s, Self-employed and Energy.

J.-F. Toubeau is a post-doctoral research fellow of the National Fund of Scientific Research (FNRS) within the "Power Systems and Markets Research Group", University of Mons, Belgium.

J. Bottieau, Z. De Grève and F. Vallée are with the same research group.

K. Bruninx is a post-doctoral research fellow of the Flanders Research Foundation (FWO) (grant no. 12J3320N) at the University of Leuven (KU Leuven) Energy Institute, TME Branch (Energy Conversion), B-3001 Leuven, Belgium) and EnergyVille, B-3600 Genk, Belgium.

$R^{\mathrm{u}}, R^{\mathrm{d}}$ Upward (u) and downward (d) reserve requirements, MW.

$x_t^{\mathrm{u}}, x_t^{\mathrm{d}}$ Raw signal of upward (u) and downward (d) reserve activation at time t, MW.

$\tilde{e}_t^{\mathrm{act,u/d}}$ Uncertain upward (u) and downward (d) ESS-based reserve activation until time t, MWh.

$\tilde{\xi}_{l,t}^{\mathrm{u}}, \tilde{\xi}_{l,t}^{\mathrm{d}}$ Uncertain upward (u) and downward (d) amount of balancing energy activated in level l until time t, MWh.

I. Introduction

In the context of the decarbonization of the power sector, energy storage systems (ESS) may play an important role by accommodating high shares of intermittent generation from renewable energy sources (RES). Indeed, their ability to bidirectionally exchange energy with the power system can cost-effectively mitigate the temporal and spatial mismatches between electricity generation and consumption, thereby contributing to the reliable operation of the grid [1].

However, capitalizing on the full value of the ESS flexibility in competitive electricity markets is a challenging task, which requires identifying the best trade-off between different revenue streams, while respecting the ESS technical constraints and the markets' requirements [2]. Typical revenue streams for merchant ESS owners originate from (i) price arbitrage in day-ahead wholesale energy markets and (ii) the provision of ancillary services such as operating reserves [3]. In this context, many authors have studied the behavior of ESS owners participating in joint energy and reserve markets [4]-[7]. However, these works do not consider the potential risk associated with the uncertain activation of reserves in real-time. Indeed, the ESS bidding strategy is not only constrained by the installed capacity (MW) and ramping abilities (MW/min) as is the case for conventional generation, but also by the storage capacity (MWh). Failing to properly anticipate the impact of the uncertain activation of scheduled reserve capacity on the storage content may thus result into overly optimistic bidding strategies, i.e., offering reserve capacity that the ESS owner is unable to deploy when requested. This may result in costly real-time balancing penalties and/or a temporary exclusion from participation in reserve markets.

Moreno et al. [8] propose a formulation that attempts ensuring the availability of reserve capacity offered by ESS. However, the impact of reserve activation on the energy capacity constraints is modeled on individual time steps and, consequently, the aggregated impact on the energy content when the reserve is activated in successive time periods is not considered. Hence, this framework does not ensure the availability of ESS-based reserves in a multi-period scheduling problem. To overcome this issue, reserve deployment is explicitly considered in [9], using an average activation rate at each time step. This deterministic procedure does not guarantee that the resulting scheduling is feasible when the actual reserve activation deviates from its mean value. In the same vein, the energy requirement is satisfied in expectation in [10], where the anticipated activation of reserves is represented through different reserve activation scenarios. These approaches [9]-[10] potentially lead to overly optimistic strategies that do not guarantee the real-time availability of the scheduled reserve capacity [11]. Conversely, explicitly ensuring that the energy constraints are respected in each scenario individually comes at a significant calculation cost [12]. An interesting alternative consists in ensuring the availability of energy for the full deployment of the scheduled reserve capacity over the scheduling horizon in a deterministic setting [13]-[15], but this conservative strategy may significantly limit the ESS owner opportunities in reserve capacity and other markets.

In this paper, we propose a novel methodology to integrate the real-time balancing stage into the day-ahead scheduling problem of a merchant ESS that jointly participates in energy, reserve capacity and balancing markets. The proposed model relies on [16]-[17], in which the expected profit secured in the balancing stage is internalized into the day-ahead decision problem under the form of probabilistic constraints. The resulting model considers the expected profit from reserve allocation and activation in a computationally efficient formulation. The contributions of our work are threefold.

Firstly, we complement the models first introduced in [16]-[17] with a data-driven probabilistic representation of the energy actually deployed at the balancing stage, which allows to properly estimate the impact of the reserve activation on the ESS energy content. This is achieved by constructing time-dependent distributions of the cumulative amount of reserves deployed over time. Results in the case study (Section III-B) demonstrate that the improved data-driven representation of the balancing actions leads to a 9% increase in profit compared to the worst-case scenario assuming the full activation of reserves (used in [16]-[17]). As such, this framework manages, at the level of the strategic player, the feasibility of activating the ESS-based reserves, while avoiding the need to rely on computationally intensive two-stage stochastic programming techniques. In addition, we bypass the need of generating an adequate set of scenarios that capture the volume, temporal correlation and probability in reserve activation [18], which is highly challenging even when considering the advent of scenario reduction techniques [19].

Secondly, by directly modeling the balancing uncertainty through distributions instead of scenarios, the proposed model offers, for the first time, a natural way of accurately capturing both the minute-by-minute variability in the required balancing energy and the merit order-based activation of reserves (in which the cheapest reserve providers are activated first, as recently advocated by the European Commission [20]). Outcomes from our case study show that disregarding these effects may falsely lead the ESS owner into believing that its schedule fully satisfies the storage content requirements, resulting in costly penalties for non-delivery. We exploit balancing signals with a one minute resolution to quantify the balancing energy needed across the scheduling horizon, as a function of the position in the merit order.

Thirdly, we further exploit the distributional representation of the balancing stage to implement a risk-aware formulation that defines probabilistic guarantees on the real-time feasibility of the ESS schedule. Based on the quantiles of the constructed distributions, we develop a continuous linear approximation of these chance constraints. This avoids the computationally

intensive solution consisting in approximating the non-convex probabilistic constraints with a large number of scenarios [21], as well as the use of complex reformulations [22]-[24]. Moreover, in contrast to [25], in which the ESS technical limits are expressed as chance constraints for a single time step, our approach allows explicitly considering the day-ahead trade-off between offering more reserves and ensuring the feasibility of their real-time delivery over the whole scheduling horizon. As illustrated in our case study, the risk-aware formulation allows a profit-maximizing trade-off between more aggressive bidding strategies and the financial penalties from the inability to comply with the day-ahead schedule.

An interesting feature of the proposed approach is that it effectively decouples the representation of the uncertain profit in the balancing market from the constraints ensuring the real-time availability of ESS-based operating reserves. The resulting framework is embedded within a bi-level model that reflects the relationship between the energy storage owner (in the upper level) and the market clearing (in the lower level) [26], [27]. We consider a linear representation of the market clearing, limiting the behavior of competing technologies to price-quantity bids. However, it is important to notice that our work can be seamlessly combined with [28], which successfully internalizes unit commitment constraints and non-convex cost structures in the lower level problem. Alternatively, it should be noted that other approaches, based on learning policies, can also be used to improve the representation of strategic behavior of market players [29], [30]. In that regard, the proposed data-driven optimization strategy also allows connecting traditional model-based formulations with the emerging field of fully data-driven approaches. In the same vein, the proposed framework can be seen as an essential building block to study other kinds of games, such as a Nash Game between strategic participants in an oligopolistic market [31]-[33]. Indeed, these games are often casted as equilibrium problems with equilibrium constraints (EPECs). Solving these EPECs requires finding a Nash equilibrium among a set of strategic actors, such that improving models governing the strategic decision of a single actor (in our case through a more accurate and computationally efficient formulation of the balancing stage) directly enhances the multi-leader game.

The presented framework may be directly integrated in the day-to-day decision making process of a ESS owner, or may be leveraged by regulators to detect market power abuse. Indeed, the bi-level model is well-suited to represent strategic behavior of ESS owners, which may be more likely to exercise market power than conventional assets. Regulators may have limited information on the state of the asset (e.g., how much energy is stored, at what cost it was charged), such that may be challenging to detect, e.g., strategic withholding of capacity.

The rest of the paper is organized as follows. In Section II, we present the risk-aware formulation of the ESS scheduling in joint energy, reserve capacity and balancing markets, with a focus on the data-driven representation of the real-time balancing stage. Then, the performance of the model is discussed in a case study (Section III), including a comparison with a scenario-based method. Finally, conclusions are formulated.

II. Day-ahead scheduling of energy storage

In Europe, the energy-only and reserve capacity markets are cleared sequentially in day-ahead (DA) via independent auctions [34]. The reserve capacity market is typically cleared shortly before the energy market, and the committed reserve capacity needs to be continuously available during the contracting period [34]. In case of real-time (RT) system imbalance (arising from forecast errors and unexpected events [35]), the procured reserves are activated according to the merit order, i.e., balancing offers are activated in ascending order of activation costs, until the system frequency is restored [36].

In this context, our objective is to develop a probabilistic representation of the uncertain balancing outcome to better inform the DA scheduling problem of ESS owners. As represented in Fig. 1, we leverage empirical probability density functions (PDFs) based on the historical observations of the activation of reserves x_t (which can be decomposed into its upward x_t^{u} and downward x_t^{d} components) at the system level.

Distinct PDFs are constructed for each hour $t \in \mathcal{T}$ to differentiate the fluctuating conditions during the day, such as an increased variability in peak periods [37], [38]. To integrate the distributional information in a computationally efficient manner in the day-ahead decision problem of the ESS owner, the up- and downward reserve requirements R^{u} and R^{d} are each split into L uniform intervals (or levels), following [16]-[17]. As discussed in Section III-A, the number of reserve levels L is selected based on a compromise between the calculation time and the accuracy in estimating the balancing revenues. The probability of reserve activation $P_{l,t}^{\mathrm{u/d}}$ depends on the level l, which reflects the position in the merit order. As depicted in Fig. 1, this information is captured by integrating the PDF, based on the past values of reserve activation x_t, between the level's bounds $A_{l-1}^{\mathrm{u/d}}$ and $A_l^{\mathrm{u/d}}$.

$$P_{l,t}^{\mathrm{u/d}} = \int_{A_{l-1}^{\mathrm{u/d}}}^{A_l^{\mathrm{u/d}}} p(x_t)\,\mathrm{d}x_t \tag{1}$$

The distributional information on the reserve activation is used by the ESS owner to compute its expected profit from the RT activation of balancing reserves, while modeling the clearing of the balancing market. It should be noted that the feasibility of the ESS schedule is enforced separately using chance constraints (Section II-A2). The resulting Stackelberg game is casted as a bi-level model, characterized by (i) an upper-level problem (Section II-A) reflecting the decision procedure of the ESS owner, who aims to define an optimal trade-off between participating in DA energy and reserve markets,

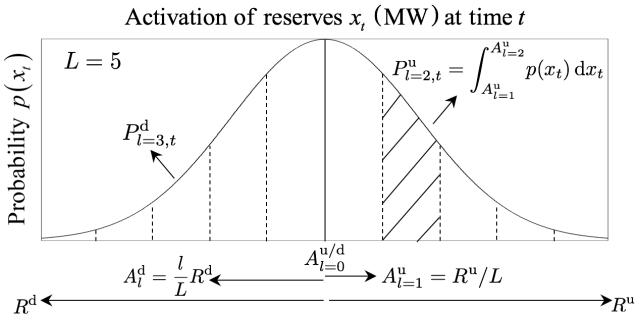

Fig. 1. Probability of activating reserves x by level $l \in \mathcal{L}$ at time $t \in \mathcal{T}$.

in view of the uncertain outcome of the RT balancing market, and (ii) a lower-level problem (Section II-B) that simulates the joint clearing of these three markets, as performed by the market operator.

A. Upper-level problem

The ESS maximizes its profit (Eq. 2) by optimally allocating capacity between (i) the DA energy market to perform arbitrage, i.e., charging p_t^{ch} when prices are low and discharging p_t^{dis} during peak prices, (ii) the DA reserve capacity market, i.e., profit from the provision of upward $\{u_t^{\mathrm{ch}}, u_t^{\mathrm{dis}}\}$ and downward $\{d_t^{\mathrm{ch}}, d_t^{\mathrm{dis}}\}$ reserve capacity, and (iii) the RT balancing market, i.e., the probability-weighted profit (Fig. 1) from the RT activation of balancing reserves per volume level l $\{ua_{l,t}^{\mathrm{ch}}, ua_{l,t}^{\mathrm{dis}}, da_{l,t}^{\mathrm{ch}}, da_{l,t}^{\mathrm{dis}}\}$. These contributions depend on the market clearing prices and quantities, which arise from the lower-level problem (Section II-B).

$$\begin{aligned}\max \sum_{t\in\mathcal{T}} \Bigg[& \underbrace{-(\lambda_t^{\mathrm{e}} + C^{\mathrm{ch}})p_t^{\mathrm{ch}} + (\lambda_t^{\mathrm{e}} - C^{\mathrm{dis}})p_t^{\mathrm{dis}}}_{\text{(i)}} \\ & + \underbrace{\lambda_t^{\mathrm{u}}\left(u_t^{\mathrm{dis}} + u_t^{\mathrm{ch}}\right) + \lambda_t^{\mathrm{d}}\left(d_t^{\mathrm{dis}} + d_t^{\mathrm{ch}}\right)}_{\text{(ii)}} \\ & + \sum_{l\in\mathcal{L}} \underbrace{P_{l,t}^{\mathrm{u}}(\lambda_t^{\mathrm{ua}} + C^{\mathrm{ch}})ua_{l,t}^{\mathrm{ch}} + (\lambda_t^{\mathrm{ua}} - C^{\mathrm{dis}})ua_{l,t}^{\mathrm{dis}}}_{\text{(iii)}} \\ & + \sum_{l\in\mathcal{L}} \underbrace{P_{l,t}^{\mathrm{d}}(\lambda_t^{\mathrm{da}} - C^{\mathrm{ch}})da_{l,t}^{\mathrm{ch}} + (\lambda_t^{\mathrm{da}} + C^{\mathrm{dis}})da_{l,t}^{\mathrm{dis}}}_{\text{(iii)}} \Bigg]\end{aligned} \tag{2}$$

Practically, the strategic agent relies on price-quantity bids, through which it is able to withhold power capacity and to express its willingness to sell/buy via the price component of the bid $\hat{o}_t$. The technical feasibility of the non-negative energy and reserve offers are enforced by (3)-(7). The ESS owner can offer upward reserves either by charging less or discharging more, and downward reserve capacity by charging more or discharging less, than its scheduled power.

$$\hat{d}_t^{\mathrm{dis}} \leq \hat{p}_t^{\mathrm{dis}} \quad \forall t \tag{3}$$

$$\hat{p}_t^{\mathrm{dis}} + \hat{u}_t^{\mathrm{dis}} \leq \overline{P}^{\mathrm{dis}} \quad \forall t \tag{4}$$

$$\hat{u}_t^{\mathrm{ch}} \leq \hat{p}_t^{\mathrm{ch}} \quad \forall t \tag{5}$$

$$\hat{p}_t^{\mathrm{ch}} + \hat{d}_t^{\mathrm{ch}} \leq \overline{P}^{\mathrm{ch}} \quad \forall t \tag{6}$$

$$\hat{o}_t^{\mathrm{ch}}, \hat{o}_t^{\mathrm{dis}}, \hat{o}_t^{\mathrm{ch,u}}, \hat{o}_t^{\mathrm{dis,u}}, \hat{o}_t^{\mathrm{ch,d}}, \hat{o}_t^{\mathrm{dis,d}} \geq 0 \quad \forall t \tag{7}$$

Constraint (8) tracks the evolution of the ESS state-of-charge based on the ESS owner's bids and offers on the energy market. We define $\tilde{e}_t^{\mathrm{act,u}}$ and $\tilde{e}_t^{\mathrm{act,d}}$, which respectively represent the uncertain upward (9) and downward (10) ESS-based reserve activation. These terms are integrated both into (11)-(12) which ensure that the stored energy remains within the technical bounds $\underline{E}$ and $\overline{E}$, and into (13) which imposes a boundary condition on the final ESS state-of-charge (i.e., a proxy for the value of stored energy at the end of the day). Constraints (11)-(13) depend on the (uncertain) amount of reserves activated at the balancing stage. As further described hereunder, we directly map the reserve activation to the ESS state-of-charge, by representing the balancing actions through distributions $\tilde{\xi}_{l,t}^{\mathrm{u/d}} \in [0,1]$ of the cumulative amount of reserves deployed over time. To manage these distributions, we enforce the probability of not respecting storage content constraints (11)-(12) to be at most $\epsilon \in [0,1]$ (Section II-A2), and the probability to violate the target energy value at the end of the day (13) to be at most $\epsilon^{\mathrm{target}} \in [0,1]$ (Section II-A3).

$$e_t = e_{t-1} + \eta^{\mathrm{ch}} p_t^{\mathrm{ch}} - \frac{p_t^{\mathrm{dis}}}{\eta^{\mathrm{dis}}} \quad \forall t \tag{8}$$

$$\begin{aligned}\tilde{e}_t^{\mathrm{act,u}} = \sum_{l\in\mathcal{L}} \tilde{\xi}_{l,t}^{\mathrm{u}} \sum_{t'=t_{\mathrm{GCT}}}^{t} \Bigg[& \frac{\left(ua_{l,t'}^{\mathrm{dis}} - ua_{l-1,t'}^{\mathrm{dis}}\right)}{\eta^{\mathrm{dis}}} \\ & + \eta^{\mathrm{ch}}\left(ua_{l,t'}^{\mathrm{ch}} - ua_{l-1,t'}^{\mathrm{ch}}\right)\Bigg] \quad \forall t\end{aligned} \tag{9}$$

$$\begin{aligned}\tilde{e}_t^{\mathrm{act,d}} = \sum_{l\in\mathcal{L}} \tilde{\xi}_{l,t}^{\mathrm{d}} \sum_{t'=t_{\mathrm{GCT}}}^{t} \Bigg[& \frac{\left(da_{l,t'}^{\mathrm{dis}} - da_{l-1,t'}^{\mathrm{dis}}\right)}{\eta^{\mathrm{dis}}} \\ & + \eta^{\mathrm{ch}}\left(da_{l,t'}^{\mathrm{ch}} - da_{l-1,t'}^{\mathrm{ch}}\right)\Bigg] \quad \forall t\end{aligned} \tag{10}$$

$$\mathbb{P}\left(e_t - \tilde{e}_t^{\mathrm{act,u}} \geq \underline{E}\right) \geq 1 - \epsilon \quad \forall t \tag{11}$$

$$\mathbb{P}\left(e_t + \tilde{e}_t^{\mathrm{act,d}} \leq \overline{E}\right) \geq 1 - \epsilon \quad \forall t \tag{12}$$

$$\mathbb{P}\left(e_T - \tilde{e}_T^{\mathrm{act,u}} + \tilde{e}_T^{\mathrm{act,d}} \geq E^{\mathrm{target}}\right) \geq 1 - \epsilon^{\mathrm{target}} \quad \forall t \tag{13}$$

Since the ESS owner needs to solve the scheduling problem at the gate closure time t_{GCT}, i.e., 12 hours before the first hour of delivery t_0, one should account for the uncertain reserve activation between t_{GCT} and t_0 (for which the reserve capacity cleared by the market is known and treated as a parameter). Moreover, $\{ua_{l=0,t}^{\mathrm{dis}}, ua_{l=0,t}^{\mathrm{ch}}, da_{l=0,t}^{\mathrm{dis}}, da_{l=0,t}^{\mathrm{ch}}\}$ are set equal to 0 by definition.

It should be noted that the model (8)-(10) presents an ideal and generic formulation of a storage system [39]. However, more detailed storage models can also be considered, including effects such as aging [40]-[41] or the dependency of the available output capacity on the ESS state-of-charge [42]-[43]. The main challenge in the context of the problem at hand is to properly account for the relation between the ESS state-of-charge and (i) the available output power and (ii) degradation effects (e.g., for Li-ion batteries). Since the real-time energy content is – by definition – stochastic, we rely on an estimated state-of-charge trajectory based on the mean activation of the scheduled reserves over the day to capture the relation between the state-of-charge and the available output capacity and aging effects. The same strategy is applied to control the target state-of-charge at the end of the day (Section II-A3). The resulting formulation is provided in Appendix, and the impacts of these constraints on model outcomes are further discussed in the case study (Section III-D).

Before we elaborate on chance constraints (11)-(12) (Section II-A2), we expose how the model deals with the uncertain, merit order-based activation of ESS-based reserves.

1) ESS-based reserve activation: The probabilistic guarantee on the RT availability of the reserves (11)-(12) should reflect a trade-off between (i) the profits in energy, reserve capacity and balancing markets and (ii) real-time penalties for non-delivery of scheduled reserve capacity. A naive approach

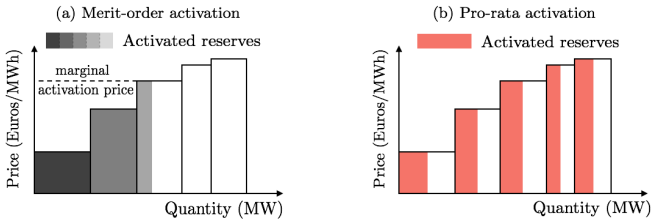

Fig. 2. Clearing of the balancing market (in which offers are ranked in economic order), with (a) the merit-order activation of reserves, and (b) the pro-rata scheme where all offers are jointly activated.

would be to set $\tilde{\xi}^{\mathrm{d}}_{l,t}$ and $\tilde{\xi}^{\mathrm{u}}_{l,t}$ to 1. This implies that, if a storage unit offers (in DA) 1 MW of upward reserve for the 24 hours of the next day, 24 MWh of stored energy must be fully reserved for RT balancing purposes at the end of the scheduling horizon [13]-[15]. However, in practice, the implicitly assumed worst-case scenario of consecutive upward or downward reserve activation in the example above is extremely unlikely. The required balancing energy falls in a much narrower range, as illustrated below.

The actual balancing requirements associated with each reserve provider $l \in \mathcal{L}$ depends on the reserve activation policy (Fig. 2). In that regard, the European Commission has recently called for *merit order-based* activation of reserves, in which reserves are activated in economic order until the system balance is restored (Fig. 2a). In this system, cost-efficient resources ($l = 1$) are more frequently activated than the more expensive offers located higher in the merit order, which may have a significant impact on the activation rates of different reserve providers. In contrast, affine control policies [21]-[22] entail that reserve providers react according to a predefined policy to a system imbalance, independent from the size of the imbalance or their position in the merit order (Fig. 2b).

In addition to the activation policy, it is also important to properly represent the sub-hourly dynamics of the balancing signal. Indeed, scenario-based approaches often make use of aggregated hourly or 15-minute activation rate [9]-[12], which may lead to improper representations of the required balancing energy. To illustrate this effect, we show the actual variability of the real-time activation of upward secondary reserves x^u_t in Fig. 3, using one minute-sampled data during 6 consecutive hours of the 1st January 2019. These data come from Elia, the Belgian transmission system operator [44]. The position in the merit order is differentiated by defining five reserve levels ($L = 5$). The impact of neglecting the balancing dynamics is highlighted via the hourly-averaged signal (where intra-hour fluctuations are averaged into a single value). We observe that this averaging solution yields an ill-representation of individual offers, e.g., by neglecting the contributions of offers higher up in the merit order.

To quantify the effects of both intra-hour variability and the merit-order based activation of reserves, we compute (over the year 2018) how the upward balancing energy is distributed among the $L = 5$ levels of the merit order. The outcomes for (i) the merit-order activation (accounting for the dynamics of the balancing signal), (ii) the pro-rata scheme, and (iii) the hourly activation rate, are shown in Fig. 4. In the raw balancing signal, 40% of the balancing energy is provided by the 20% most cost-efficient resources ($l = 1$), while the 20% most

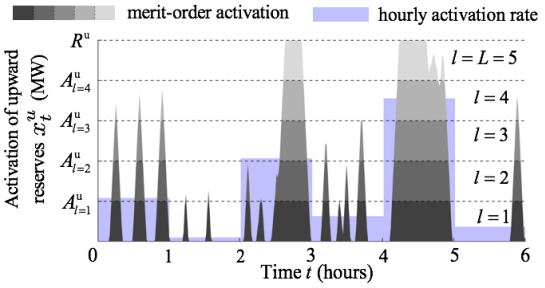

Fig. 3. Activation of upward secondary reserves x^u_t during 6 hours of the 1st January 2019, where resources $l \in \mathcal{L}$ are activated in ascending order of cost-effectiveness until the system imbalance is compensated.

expensive offers ($l = 5$) only contribute to 8% of the needed upward balancing energy. As observed in Fig. 3, an hourly-averaged value systematically overestimates the contribution of cost-efficient resources ($l = 1$), while underestimating the energy deployed by the most expensive offers ($l \geq 3$). The pro-rata system, where all reserve providers equally contribute to the balancing task, leads to the opposite mis-representation. Hence, to accurately model the required balancing energy, it is necessary to account for both the sub-hourly dynamics and the activation policy of the balancing signal.

Therefore, in this paper, we leverage historical balancing data sampled with a one-minute resolution to fully account for the intra-hour variability of the balancing signal and the merit order-based activation of reserves. Raw data are differentiated between L balancing levels, and then aggregated per volume level l. To that end, we compute the accumulated balancing energy $E^{\mathrm{u/d}}_{i,l,t}$ of day i in level l between t_{GCT} and time t. This quantity is normalized with respect to the total reserve requirements, such that it varies between 0 (if no reserve activation) and 1 (in case of full activation over the horizon):

$$E^{\mathrm{u/d}}_{i,l,t} = \frac{1}{t - t_{\mathrm{GCT}}} \int_{\tau=t_{\mathrm{GCT}}}^{\tau=t} \frac{1}{\Delta l} \int_{p=A^{\mathrm{u/d}}_{l-1}}^{p=A^{\mathrm{u/d}}_{l}} x^{\mathrm{u/d}}_{i,\tau} \, \mathrm{d}p\mathrm{d}\tau \quad (14)$$

where Δl is the width of the reserve levels, and $x^{\mathrm{u/d}}_{i,\tau}$ is the raw signal of reserve activation of day i at time τ (see Fig. 3 for upward activation). By repeating this operation for all days of the database, we can build (for each level) a time-dependent probabilistic representation of the cumulative energy $\tilde{\xi}^{\mathrm{u/d}}_{l,t} \in [0, 1]$ deployed at the balancing stage among successive periods, thereby linking through time the individual distributions of Fig. 1. In Fig. 5, we show the distribution of the cumulative upward secondary reserve activation for extreme levels $l = 1$ and 5. As a benchmark, we also represent (in dashed lines) the worst-case scenario $\xi^{\mathrm{u}}_{l,t} = 1$ of full reserve activation over time, thus illustrating the conservativeness of this assumption.

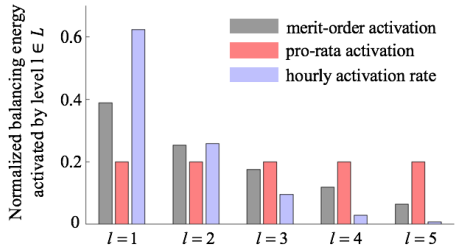

Fig. 4. Repartition of the total balancing energy over the year 2018 between the $L = 5$ levels, for the different assumptions on the reserve activation.

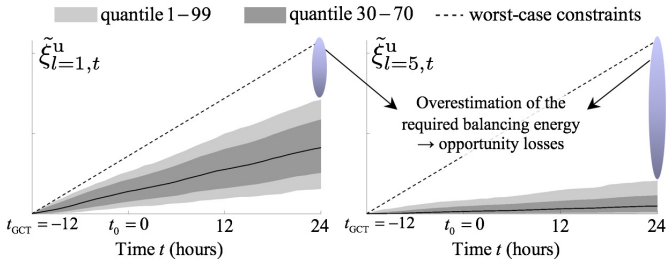

Fig. 5. Probability distribution of the cumulative balancing energy over the scheduling horizon for the two outer levels in the merit order. The worst-case scenario of full activation of reserves over time represents the limit $\xi^{u}_{l,t} = 1$.

2) Chance constraints controlling the feasibility of the ESS-based schedule: In this work, chance constraints are used to relax the worst-case constraints enforcing the availability of reserves in real time (Fig. 5). This is achieved by exploiting the distributions of the activated reserves $\tilde{\xi}^{d}_{l,t}, \tilde{\xi}^{u}_{l,t} \in [0,1]$ in Eq. (11)-(12).

Practically, we exploit the fact that the decision variables $\mathbf{x}_t = \{e_t, ua^{dis}_{l,t}, ua^{ch}_{l,t}, da^{dis}_{l,t}, da^{ch}_{l,t}\}$ are affinely dependent on the random vector $\tilde{\boldsymbol{\xi}}_t \in \left\{\tilde{\xi}_{1,t}, ..., \tilde{\xi}_{L,t}\right\} \in \mathbb{R}^L$, such that chance constraints (11)-(12) can be rewritten in a generic way as:

$$\mathbb{P}\left(\mathbf{a}^\top \tilde{\boldsymbol{\xi}} \leq b\right) \geq 1 - \epsilon \tag{15}$$

where the time indices are omitted for clarity. We define the vector $\mathbf{a} = \mathbf{A_1 x} + \mathbf{a_2}$ and scalar $b = \mathbf{b_1}^\top \mathbf{x} + b_2$, with $\{\mathbf{a}, \mathbf{a_2}\} \in \mathbb{R}^L$, $\mathbf{A_1} \in \mathbb{R}^{L \times X}$, $\{b, b_2\} \in \mathbb{R}$ and $\mathbf{b_1} \in \mathbb{R}^X$.

In this work, we substitute the left-hand side of Eq. (15) with a deterministic expression:

$$\mathbb{P}\left(\mathbf{a}^\top \tilde{\boldsymbol{\xi}} - b \leq 0\right) \geq 1 - \epsilon \Leftrightarrow \mathrm{VaR}_{1-\epsilon}\left(\mathbf{a}^\top \tilde{\boldsymbol{\xi}} - b\right) \leq 0 \tag{16}$$

where the value-at-risk $\mathrm{VaR}_{1-\epsilon}$ is the $(1-\epsilon)$-quantile of the one-dimensional distribution defined by $\mathbf{a}^\top \tilde{\boldsymbol{\xi}} - b$. Hence, when $L = 1$, the chance constraint (15) can be approximated by an equivalent linear problem

$$\mathbf{a} \cdot q_{1-\epsilon} - b \leq 0 \tag{17}$$

where $q_{1-\epsilon}$ is the $(1-\epsilon)$-quantile of the unidimensional $\tilde{\boldsymbol{\xi}}$, i.e., $q_{1-\epsilon} = \inf\left\{y \in \mathbb{R}^+ : \mathbb{P}\left(\tilde{\boldsymbol{\xi}} \leq y\right) \geq (1-\epsilon)\right\}$.

In a multi-dimensional setting, i.e., when $L > 1$, the problem is more difficult to solve since the dependence structure among variables, and thus the feasible region of the chance constraint, is typically non-convex. Here, we propose an extension of the univariate case (17), in which we use the marginal distribution functions (associated with each level) to approximate chance constraint (15). As depicted in Fig. 6 for $l = \{1, 5\}$, we can replace the marginal distributions $\tilde{\xi}^{u/d}_{l,t}$ by their quantile $q^{u/d}_{1-\epsilon_l,t}$. Note that this approach does not imply any assumption on the form of the distribution, i.e., the method only requires that the quantiles can be defined, which is done here based on historical data.

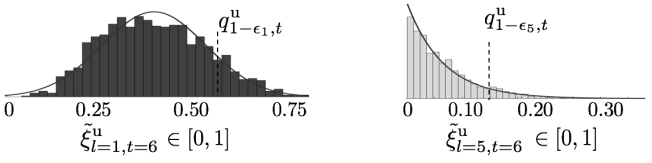

Fig. 6. Empirical probability distribution of the accumulated balancing energy $\tilde{\xi}^{u}_{l,t} \in [0,1]$ activated in levels $l \in \{1,5\}$ at time $t = 6$. The solid line depicts a kernel density estimation of the empirical distribution. In accordance with Fig. 5, we see that the amount of energy activated in level $l = 1$ (average activation of 40 % of the total requirements) is much larger than for $l = 5$ (average activation of 12 %). The dotted vertical lines show the quantiles $q^{u}_{1-\epsilon_l,t}$ defining the frontier of the feasible region of the chance constraints.

The quantiles are selected to ensure a conservative approximation of chance constraints (11)-(12), such that the resulting ESS schedule is on the safe side regarding its (ex-post) reliability (Section III). Practically, this compliance with the user-defined risk-attitude ϵ is achieved by imposing that the sum of violation probabilities ϵ_l in each of the L dimensions of $\tilde{\boldsymbol{\xi}}$ does not exceed ϵ, i.e. $\sum_{l \in \mathcal{L}} \epsilon_l \leq \epsilon$.

Using historical data, this strategy is illustrated in Fig. 7 for $\epsilon = 0.2$. The scatter plot illustrates the accumulated balancing energy associated to both extreme levels (i.e. $l = 1$ and 5) of the 5-dimensional uncertainty $\tilde{\xi}^{u}_{l,t}$. The targeted risk-level ϵ is equally distributed among dimensions, by fixing $\epsilon_l = \epsilon/L = 0.04 \ \forall l = \{1, ..., 5\}$. The resulting quantiles $q^{u}_{1-\epsilon_l,t}$ define the feasible region of the chance constrained problem. For this specific case, the proposed method provides an in-sample guarantee of 0.12. The increased conservativeness with respect to the desired $\epsilon = 0.2$ arises from the correlation between different dimensions. Indeed, our strategy may lead to "double counting" (scenarios in the zone II of Fig. 7): realizations that are excluded based on the quantile in one dimension, can also be accounted for in other dimensions.

In summary, we can express the resulting continuous and linear approximation of chance constraints (11)-(12), as follows, here illustrated for Eq. (11):

$$e_t - \sum_{l \in \mathcal{L}} q^{u}_{1-\epsilon_l,t} \sum_{t'=t_{GCT}}^{t} \left[\frac{\left(ua^{dis}_{l,t'} - ua^{dis}_{l-1,t'}\right)}{\eta^{dis}} + \eta^{ch}\left(ua^{ch}_{l,t'} - ua^{ch}_{l-1,t'}\right) \right] \geq \underline{E} \ \forall t \tag{18}$$

Note that this approach is typically more computationally efficient than traditional scenario-based approaches for chance-constrained programming, which requires duplicating the chance constraints by scenario and adding binary variables to indicate which scenario-specific constraints are to be satisfied or violated [45]. An alternative for taking decisions accounting for security consists in relying on conditional probability distributions determined by measurements [46].

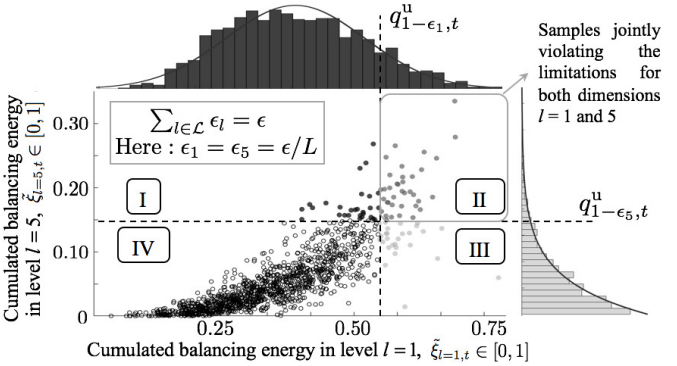

Fig. 7. Bivariate distribution of the cumulated balancing energy $\tilde{\boldsymbol{\xi}}$ between t_{GCT} and $t = 6$ for levels $l = 1$ and 5. The probabilistic guarantees (on the availability of reserves) are expressed under the form of quantiles q_{ϵ_l}, which define the frontier between the feasible region of chance constraints (zone IV), and the ϵ-zone where constraint violation is tolerated (zones I-II-III).

This framework is shown to return an approximation of the exact feasibility region in the decision space. In the same vein, distributionally robust optimization [47]-[50] can be used to hedge against ambiguity in the distribution of $\tilde{\boldsymbol{\xi}}$.

3) Chance constraints controlling the compliance with the target value of state-of-charge at $t = T$: We impose that the storage system's state of charge (13) at the end of the horizon $t = T$ accounts for the mean activation of scheduled reserves over the day [51], i.e., $\tilde{\xi}^{\mathrm{u/d}}_{l,T} = q^{\mathrm{u/d}}_{\epsilon_l=0.5,T}\,\forall l$.

B. Lower-level problem

In the lower-level (LL), the ESS forms a deterministic estimation of the energy and reserve markets clearings, whereas the balancing stage is cleared for different levels $l \in \mathcal{L}$ of imbalances, each with their probability of occurrence $P^{\mathrm{u/d}}_{l,t}$. The real-time balancing market is not explicitly modeled as a sequential stage after the day-ahead trading floor, but it is internalized into the day-ahead model under the form of probabilistic constraints. This implies that actors perform arbitrage between markets, which leads to price convergence, as observed in real-life markets [52]. Also, the interaction between congestion management and balancing is not considered in the model. However, in the case study at hand (Section III), this is not a strong assumption: recent studies show that the amount of redispatching due to congestion in the Belgian system is limited (around 0.08 % of the annual load) [53].

The problem is constrained by the ESS owner's strategic bids, while other market participants are assumed to be price-takers. Conventional units offer their capacities at average generation cost, and renewable energy is offered at 0 €/MWh. We assume that the demand bids are offered at the price cap c_j to ensure they are accepted. However, this value of loss load can be easily differentiated to better reflect the price elasticity of different types of loads.

$$\begin{aligned}\min \sum_{t\in\mathcal{T}} \Bigg[& \hat{o}^{\mathrm{dis}}_t p^{\mathrm{dis}}_t - \hat{o}^{\mathrm{ch}}_t p^{\mathrm{ch}}_t + \sum_{g\in\mathcal{G}} C_g p_{g,t} - \sum_{j\in\mathcal{J}} C_j p_{j,t} \\ & + \hat{o}^{\mathrm{dis,u}}_t u^{\mathrm{dis}}_t + \hat{o}^{\mathrm{ch,u}}_t u^{\mathrm{ch}}_t + \hat{o}^{\mathrm{dis,d}}_t d^{\mathrm{dis}}_t + \hat{o}^{\mathrm{ch,d}}_t d^{\mathrm{ch}}_t \\ & + \sum_{g\in\mathcal{G}} \left(C^{\mathrm{u}}_g u_{g,t} + C^{\mathrm{d}}_g d_{g,t}\right) + \sum_{j\in\mathcal{J}} C^{\mathrm{u}}_j u_{j,t} \\ & + \sum_{l\in\mathcal{L}} P^{\mathrm{u}}_{l,t} \Bigg(\hat{o}^{\mathrm{dis}}_t ua^{\mathrm{dis}}_{l,t} + \hat{o}^{\mathrm{ch}}_t ua^{\mathrm{ch}}_{l,t} \\ & \qquad + \sum_{g\in\mathcal{G}} C_g ua_{g,l,t} + \sum_{j\in\mathcal{J}} C_j ua_{j,l,t} \Bigg) \\ & - \sum_{l\in\mathcal{L}} P^{\mathrm{d}}_{l,t} \Bigg(\hat{o}^{\mathrm{dis}}_t da^{\mathrm{dis}}_{l,t} + \hat{o}^{\mathrm{ch}}_t da^{\mathrm{ch}}_{l,t} + \sum_{g\in\mathcal{G}} C_g da_{g,l,t} \Bigg) \Bigg] \end{aligned} \tag{19}$$

All clearing prices are determined based on the marginally accepted offer, and each price is thus equal to the dual variable associated with its corresponding market clearing constraint. These dual variables are indicated after each constraint, respectively for the balances in the DA energy (20), DA reserve capacity (21)-(22), and RT balancing markets (23)-(24).

$$\sum_{g\in\mathcal{G}} p_{g,t} + p^{\mathrm{dis}}_t - p^{\mathrm{ch}}_t + \sum_{w\in\mathcal{W}} p_{w,t} = \sum_{j\in\mathcal{J}} p_{j,t} \quad \forall t : \lambda^{\mathrm{e}}_t \tag{20}$$

$$\sum_{g\in\mathcal{G}} u_{g,t} + u^{\mathrm{dis}}_t + u^{\mathrm{ch}}_t + \sum_{w\in\mathcal{W}} u_{w,t} + \sum_{j\in\mathcal{J}} u_{j,t} = R^{\mathrm{u}} \quad \forall t : \lambda^{\mathrm{u}}_t \tag{21}$$

$$\sum_{g\in\mathcal{G}} d_{g,t} + d^{\mathrm{dis}}_t + d^{\mathrm{ch}}_t + \sum_{w\in\mathcal{W}} d_{w,t} = R^{\mathrm{d}} \quad \forall t : \lambda^{\mathrm{d}}_t \tag{22}$$

$$\begin{aligned}\sum_{g\in\mathcal{G}} ua_{g,l,t} + ua^{\mathrm{dis}}_{l,t} + ua^{\mathrm{ch}}_{l,t} + \sum_{w\in\mathcal{W}} ua_{w,l,t} + \sum_{j\in\mathcal{J}} ua_{j,l,t} \\ = A^{\mathrm{u}}_l \quad \forall l, t : P^{\mathrm{u}}_{l,t}\lambda^{\mathrm{ua}}_{l,t}\end{aligned} \tag{23}$$

$$\sum_{g\in\mathcal{G}} da_{g,l,t} + da^{\mathrm{dis}}_{l,t} + da^{\mathrm{ch}}_{l,t} + \sum_{w\in\mathcal{W}} da_{w,l,t} = A^{\mathrm{d}}_l \;\forall l, t : P^{\mathrm{d}}_{l,t}\lambda^{\mathrm{da}}_{l,t} \tag{24}$$

Constraints (25)-(26) ensure that the scheduled ESS output and reserve capacity respect the owner's bids. Likewise, Eq. (27)-(30) enforce that all activated reserves in the balancing market are effectively procured in the DA reserve market and that their volume does not exceed the owner's bids.

$$u^{\mathrm{ch}}_t \le p^{\mathrm{ch}}_t \le \hat{p}^{\mathrm{ch}}_t \quad \forall t \tag{25}$$

$$d^{\mathrm{ch}}_t \le p^{\mathrm{ch}}_t \le \hat{p}^{\mathrm{ch}}_t \quad \forall t \tag{26}$$

$$ua^{\mathrm{ch}}_{L,t} \le u^{\mathrm{ch}}_t \le \hat{u}^{\mathrm{ch}}_t \quad \forall t \tag{27}$$

$$ua^{\mathrm{dis}}_{L,t} \le u^{\mathrm{dis}}_t \le \hat{u}^{\mathrm{dis}}_t \quad \forall t \tag{28}$$

$$da^{\mathrm{ch}}_{L,t} \le d^{\mathrm{ch}}_t \le \hat{d}^{\mathrm{ch}}_t \quad \forall t \tag{29}$$

$$da^{\mathrm{dis}}_{L,t} \le d^{\mathrm{dis}}_t \le \hat{d}^{\mathrm{dis}}_t \quad \forall t \tag{30}$$

Technical limits are enforced in (31)-(32) for conventional units, and in (33)-(34) for RES production. Upward RES-based reserve requires scheduling less RES than the deterministic forecast $\overline{P}_{w,t}$, while a downward reserve contribution consists in real-time curtailment with respect to the day-ahead schedule. The flexibility of demand is limited by (35). This representation can be complemented with novel demand response strategies [54], [55], which are out of the scope of this paper.

$$da_{g,L,t} \le d_{g,t} \le p_{g,t}\;\forall g,t \tag{31}$$

$$ua_{g,L,t} \le u_{g,t} \le \overline{P}_g - p_{g,t}\;\forall g,t \tag{32}$$

$$da_{w,L,t} \le d_{w,t} \le p_{w,t}\;\forall w,t \tag{33}$$

$$ua_{w,L,t} \le u_{w,t} \le \overline{P}_{w,t} - p_{w,t}\;\forall w,t \tag{34}$$

$$ua_{j,L,t} \le u_{j,t} \le p_{j,t} \le D_{j,t}\;\forall j,t \tag{35}$$

The balancing market is cleared for L different levels of imbalances, where the merit order-based reserve activation is modeled by Eqs. (36)-(39). These constraints reflect that when a level is reached, the full reserve capacity (from previous levels up to its outer bound) is assumed to be activated. Integrating these constraints into the DA scheduling allows co-optimizing the DA and RT revenue streams within a *single stage* framework.

$$0 \le ua^{\mathrm{s}}_{l,t} \le ua^{\mathrm{s}}_{l+1,t} \quad \forall \mathrm{s} \in \{\mathrm{dis},\mathrm{ch}\}, l \in \{1,...,L-1\}, t \tag{36}$$

$$0 \le da^{\mathrm{s}}_{l,t} \le da^{\mathrm{s}}_{l+1,t} \quad \forall \mathrm{s} \in \{\mathrm{dis},\mathrm{ch}\}, l \in \{1,...,L-1\}, t \tag{37}$$

$$0 \le ua_{i,l,t} \le ua_{i,l+1,t} \quad \forall i \in \{g,w,j\}, l \in \{1,...,L-1\}, t \tag{38}$$

$$0 \le da_{i,l,t} \le da_{i,l+1,t} \quad \forall i \in \{g,w,j\}, l \in \{1,...,L-1\}, t \tag{39}$$

C. Summary & Solution procedure

The proposed framework is summarized in Fig. 8. An advantage of the model is that it decouples the represen-

tation of the uncertain profit in the balancing market from the constraints ensuring the real-time availability of ESS-based operating reserves. Indeed, on the one hand, the profit maximization in DA and RT markets is formulated as a single stage problem through the probabilistic representation of the RT balancing stage (Fig. 1). On the other hand, the degree of conservativeness on the feasibility of the ESS scheduling is controlled independently through chance constraints, which are guided by the uncertain activation of balancing reserves over time (Fig. 5).

To capture the strategic behavior of the ESS, the problem is formulated as a bi-level optimization problem. Solving this problem entails replacing the linear and continuous LL problem by its Karush-Kuhn-Tucker optimality conditions. The nested optimization model boils down to a single level problem that contains two types of non-linearities: (i) the UL objective function is composed of bilinear products of the LL variables, and (ii) the complementary slackness conditions associated with inequality constraints of the LL problem. The UL objective function is reformulated using the strong duality theorem, while the complementary slackness conditions are recasted as a set of mixed-integer linear constraints by introducing SOS1 variables [56]. This technique avoids the risk of an improper selection of "big-M" values [57], but at the cost of introducing a set of auxiliary SOS1 variables.

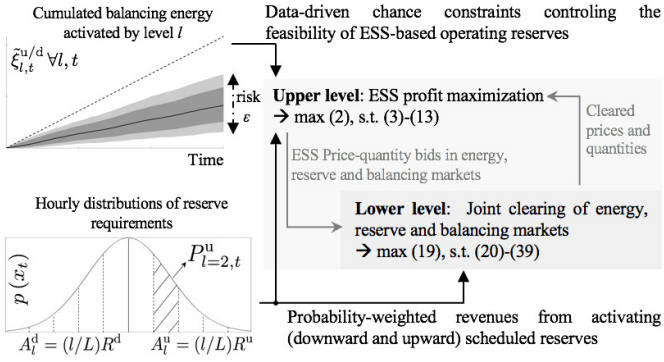

Fig. 8. Data-driven bi-level optimization framework, where we separate the representation of the balancing market (Fig. 1) from the risk-aware constraints controlling the ESS ability to provide reserves (Fig. 5).

III. Case study

In our reference setting, we study a 250 MW – 1200 MWh merchant storage unit competing in a power system inspired by the Belgian case [58]. The scheduling horizon is one day and the temporal resolution is one hour. The outcomes are studied for a specific day in which the peak demand equals 14 GW, while the lowest net demand is 6 GW. Conventional generation (18 GW) is clustered into 4 groups based on their cost characteristics (Table I). The installed wind generation is equal to 4 GW. We focus on a single reserve product, i.e., the secondary reserve or aFRR (automatic frequency restoration reserves), which must be fully delivered within a timescale of 7.5 minutes. The system reserve requirements are set to 150 MW for the upward R^{u} and downward R^{d} reserve products.

The reserve activation data for the period 2015-2018, obtained from Elia NV [44], is divided into two parts: the first one contains 75% of the samples (i.e., 3 years of data – the training set) which are used to construct the distributions feeding the optimization framework (Fig. 1 and Fig. 5), whereas the second part contains the remaining 25% of samples in order to assess the quality of the decisions (the test set). The test set is used in an ex-post Monte Carlo analysis to reveal any bias introduced by modeling assumptions [59]-[60]. We compute the actual profit that will be generated in each balancing scenario by fixing the day-ahead decisions. Any inability to comply with the day-ahead reserve schedule is penalized at 200 €/MWh. This out-of-sample analysis is, hence, performed with actual (raw) balancing outcomes (hence, without assuming any distribution), considering a one minute time resolution, such that the ex-post results accurately reflect the actual performance of the proposed formulation in case of deployment in real-life electricity and ancillary services markets.

TABLE I
Techno-economic parameters of non-strategic market actors.

Resource i	$\overline{P}_i$ (MW)	C_i (€/MWh)	C^{u}_i (€/MWh)	C^{d}_i (€/MWh)
Base	6000	20	12	0
Low mid	4000	30	10	0
Up mid	4000	40	8	0
Peak	4000	50	6	0
RES	4000	0	0	0

In Section III-A, a sensitivity analysis is performed to estimate the optimal number of levels L to model the balancing stage, in order to achieve a trade-off between computational burden and modeling accuracy. Then, we study the impact of the risk-attitude on the ESS profitability. In Section III-C, we focus on the impact of the merit order activation of reserves. Finally, we study the influence of ESS technical characteristics on the resulting bidding behavior in Section IV-D.

All models are coded in Julia/JuMP, and solved with Gurobi 8.1.1, on a 16 GB-RAM computer clocking at 3.40 GHz.

A. Scalability analysis

In this section, we analyze the effect of more accurate representation of the balancing market. To that end, we model the (uncertain) upward and downward activation of reserves with different numbers of levels $L = \{1, 3, 5, 10\}$ (i.e. the distribution of the raw balancing signal is divided into $2L$ intervals). The results are summarized in Fig. 9, where we compare (a) the ex-ante profits across all markets (expected at the end of the optimization) with the expected ex-post profit generated in the Monte Carlo out-of-sample analysis and (b) the calculation time. The simulations are carried out for a risk-averse ESS owner, who ensures feasibility of activating the offered reserve capacity in the worst-case balancing scenario in the input data, i.e., $\epsilon = 0$.

When the number of levels used to represent the balancing market is too low (here, for $L < 5$), the model tends to overestimate the probability of activating reserve capacity. This leads to bias in the ESS schedule towards offering the maximum capacity in the upward reserve market during peak periods. However, since the actual probability of activation is lower, the ex-post balancing market profit is lower. In

TABLE II
COMPARISON OF THE ESS PROFITABILITY FOR DIFFERENT APPROACHES AND DIFFERENT PROBABILISTIC GUARANTEES.

	Expected reliability (%)	Expected profit (k€)	Computation time (s)	Profit in the DA energy market (k€)	Profit in the DA reserve capacity market (k€)	Profit in the RT balancing market (k€)	Ex-post reliability (%)	Ex-post mean profit (k€)
SP with N = 10	100	33.2	75	4.8	8.4	20.0	89.7	30.4
SP with N = 50	100	29.3	735	8.0	6.1	15.2	99.3	28.9
Worst-case	100	26.3	0.8	18.9	2.0	5.8	100	26.3
Ref, ϵ = 0	100	29.1	2.7	13.5	4.4	11.2	99.7	28.7
Ref, ϵ = 0.05	95	32.0	7.3	4.0	8.2	19.8	94.3	30.8
Ref, ϵ = 0.1	90	32.6	9.6	5.5	8.1	19.0	92.7	31.3
Ref, ϵ = 0.2	80	33.5	37.0	4.3	8.7	20.5	83.7	30.3

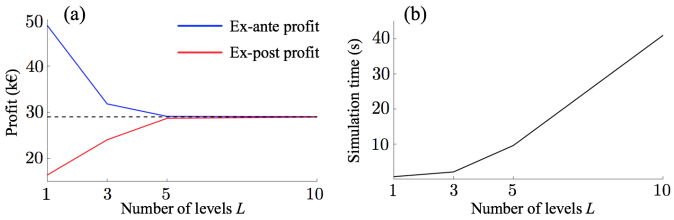

Fig. 9. Impact of the number of levels L on: (a) the ex-ante and ex-post profit across all markets, and (b) the calculation time of the optimization model.

addition, since the ESS has a limited power and energy capacity, the capacity offered in the reserve market cannot be used for arbitrage purposes, ultimately resulting in suboptimal scheduling decisions. These effects are evidently exacerbated when L = 1, where we observe that the optimization model is expecting a total profit of 48.8 k€, while it generates an expected profit 16.4 k€ in the ex-post Monte Carlo samples.

As expected, as the number of levels increases, we observe that the ex-ante and ex-post profit are converging towards the same value, which demonstrates that the model better reflects the actual market conditions. However, this gain in accuracy comes at the expense of higher calculation times, from less than 1 second when L = 1 up to 31 seconds for L = 10. This is mainly related to the size of problem. Indeed, when L = 1, the model contains approximatively 5,952 variables among which 1,512 are of SOS1 type, for a total number of 9,289 constraints. The equivalent problem considering 10 reserve levels is composed of 19,344 variables among which 4,742 are SOS1 variables, and is characterized by 29,161 equations. In the remainder of the paper, we use L = 5 as a trade-off between the calculation time and the accuracy in estimating the balancing revenues.

B. Impact of balancing energy constraints

We compare the results of three different formulations:

(i) the proposed single-stage approach (Ref) for different probabilistic guarantees on the feasibility of the real-time deployment of ESS-based reserves (Eq. (11)-(12));

(ii) the variant with conservative energy constraints (dashed line in Fig. 5), considering the full activation of reserves over the scheduling horizon, i.e., $\tilde{\xi}^{\mathrm{u/d}}_{l,t} = 1\,\forall l,t$;

(iii) a stochastic program (SP) [12] in which the uncertain balancing market outcome is represented with N = {10, 50} scenarios, which are obtained by clustering the daily sequences of the hourly-averaged energy deployed at the balancing stage. The feasibility of the ESS-based reserve dispatch is enforced in each scenario.

In Table II, we summarize the results of the numerical simulations, which include (i) the computation time and the expected profit obtained at the end of the optimization, (ii) the different contributions of the profit given by the out-of- sample analysis, i.e., the revenues from the DA energy arbitrage, DA provision of reserve capacity, and RT deployment of balancing energy. Finally, the reliability (i.e., the percentage of ex-post scenarios for which the scheduled ESS-based reserves is activated without violating the ESS constraints) and the ex-post profit are computed. The latter is estimated by taking into account the financial losses in case of non-delivered balancing energy (valued at 200€/MWh), while considering the value of stored energy at the end of the day. If the final stored energy is below the target value, the difference is penalized at the average energy procurement price on the next day.

Outcomes show that the proposed single-stage model is computationally efficient in comparison to the scenario-based alternative. For a small number of scenarios (N=10), the stochastic program requires 75 s to solve, i.e., 8 times longer than the proposed formulation with the optimal probabilistic guarantee of ϵ = 0.1. Interestingly, we see that the stochastic framework provides better performance when the number of scenarios is low (i.e. N = 10). Indeed, increasing the number of scenario (up to 50) raises the conservativeness of the solution at the expense of the expected profit, since the activation of scheduled reserve capacity must be feasible in all scenarios. Note, however, that allowing and penalizing scenario-dependent non-delivery of balancing energy in a stochastic programming framework should, in theory, yield the schedule that maximizes the expected profit, if one considers a sufficiently high number of scenarios. In this case study, the quality of the scenario-based solution remains lower than the proposed method, which can be partly explained by the loss of information incurred by the hourly-averaged scenarios, as illustrated in Fig. 4.

As expected, the worst-case energy constraints (which are robust towards the unrealistic scenario of full activation of reserves over the whole horizon) do not lead to real-time penalties. However, this conservative approach strongly tightens the storage capacity's bounds, which ultimately yields significant opportunity losses in the energy market, i.e., the energy allocated to reserves cannot be used for arbitrage purposes. This problem can be alleviated through an accurate representation of possible balancing market outcomes (Fig. 5). In this way, even when ensuring that the solution is feasible in all historical cases (by considering the worst-case scenario

in the input data, i.e., setting $\epsilon = 0$), the ESS profitability is increased by 2.4 k€ or 9.1 %.

The strategy can be further enhanced by exploiting the ESS flexibility more aggressively, i.e., with an optimal probabilistic guarantee ϵ informed by the actual probability of reserve activation. In that regard, reducing ϵ boosts the ESS participation in the upward reserve market. However, the downside of offering more capacity (which may not be fully available in real-time) is the greater risk of non-delivery. This effect is quantified by the reliability levels in Table II. Note, however, that the ex-post reliability is close to the pre-defined reliability (i.e., the one enforced in the optimization), which illustrates the effectiveness of the approach. As expected, low probabilistic guarantees (i.e., low $1 - \epsilon$ values) yield an optimistic valuation of the expected profit, and infer a high variability in the profit actually generated among ex-post scenarios. Indeed, such policies overestimate the balancing revenues (a part of the balancing energy is not delivered, and thus not rewarded) and neglect the resulting penalties. Hence, it is possible to find an optimal probabilistic guarantee ϵ, characterized by the trade-off between the profit from offering more reserves and the penalties in case of non-delivery. In our case, the best solution is achieved for $\epsilon = 0.1$, leading to an ex-post reliability of 92.7 %. Overall, less risk-averse strategies (in comparison with the scenario-based equivalent) allow increasing the profit by 900 € (from 30.4 k€ to 31.3 k€), i.e., a relative increase of approximately 3 %.

This optimal strategy in energy and reserve markets is shown in Fig. 10. The ESS unit does not operate at full (discharge) power during peak prices in order to leave a margin for providing upward reserve capacity. The ESS operates during the whole day, even during intermediate prices in the energy market (around 30 €/MWh), which enables the continuous provision of upward reserve capacity. As expected, the ESS does not provide downward reserve since such services can be more efficiently delivered by conventional generators (due to cost reductions from the associated fuel savings). Hence, the constraint (12) on the upper bound of the state-of-charge is never violated.

C. Impact of merit order-based activation of reserves

In this section, we quantify the effect of neglecting this competition effect into the DA scheduling. To that end, we use the proposed formulation, but consider a pro-rata reserve activation scheme in which all reserve providers respond proportionally to an imbalance signal. This solution is compared to the original model where the merit order activation of reserves is properly considered for the optimal strategy ($\epsilon = 0.1$) in Section III-A. In Fig. 11, we represent the reliability (%), the energy not delivered (END) when the ESS is unable to fulfill its DA schedule (MWh), and the resulting profit (k€) as given by the out-of-sample analysis.

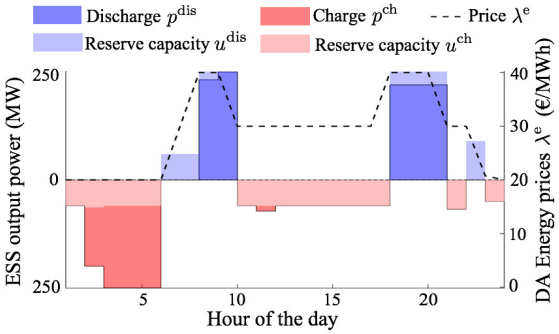

Fig. 10. Day-ahead schedule of the ESS, along with the cleared energy prices to the optimal risk-attitude $\epsilon = 0.1$.

Neglecting the merit order reserve activation systematically leads to a lower ex-post reliability than the level of probabilistic protection ϵ targeted during the optimization. Indeed, for efficient storage systems (which are able to position themselves in the beginning of the merit order), a formulation based on a pro-rata reserve activation scheme underestimates the energy actually deployed at the balancing stage. Ignoring the competition effect thereby causes undesired RT violations of the ESS operating constraints, which are translated into higher quantities of energy not delivered. This ultimately results in severe ex-post penalties, hence, lower expected profits and higher variability in profits per scenario.

D. Impact of ESS characteristics

We analyze the impact of different techno-economic characteristics of ESS on the subsequent bidding strategy by studying three different storage technologies, whose properties are given in Table III. The first unit (unit #1, which is used in previous simulations) has technical capabilities representative of gravity storage systems (such as pumped-hydro energy storage), the second one (unit #2) represents a battery system, while the third one (unit #3) has characteristics similar to those of a compressed air energy storage (CAES) system.

These three technologies are represented by the generic storage model (8)-(10). Hence, to evaluate the impact of complex dependencies between the state-of-charge, charging capabilities and aging, a more advanced model (unit #4) is introduced to mimic the actual behavior of a battery system. This model is presented in the Appendix. The (two-dimensional) nonlinear dependency between the charging power and the battery energy content is approximated through a (2 segments) piecewise linear function, as suggested in [43]. The (technology-dependent) degradation effects, which are usually assumed to be known through experimental data, is approximated via a mixed-integer linear formulation [41]. Typically, shallow cycles with high state-of-charge are relatively inexpensive, whereas the costs increase for deeper cycles starting from a lower energy content. Here, we consider a battery with capital costs of 200 €/kWh, with similar degradation characteristics as those in [41]. The optimal strategies for units #2, #3 and #4 are shown in Fig. 12. Recall that the optimal strategy for unit #1 is shown in Fig. 10.

TABLE III
TECHNICAL CHARACTERISTICS OF STORAGE SYSTEMS.

Technology	$\overline{P}^{\text{ch}}$ / $\overline{P}^{\text{dis}}$ (MW)	C^{ch} / C^{dis} (€/MWh)	$\overline{E}$ (MWh)	η^{ch} / η^{dis}
unit #1	250 / 250	2 / 2	1200	0.8
unit #2	250 / 250	2 / 2	300	0.95
units #3 - #4	150 / 250	2 / 12	1200	0.8

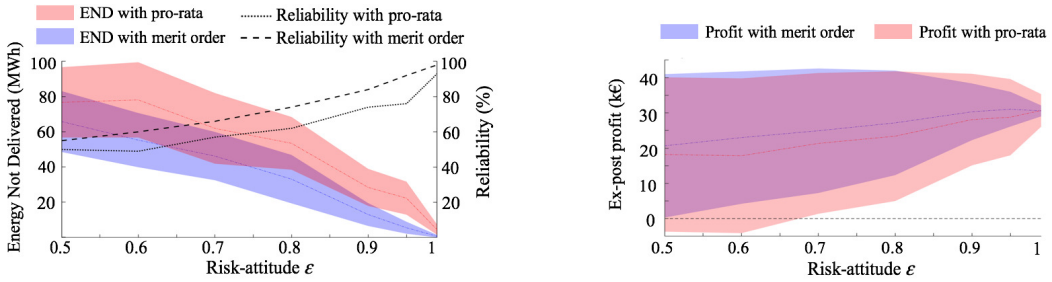

Fig. 11. Impact of the merit order activation of reserves on the energy not delivered (MWh) and expected profit (k€) for different risk-attitudes ϵ.

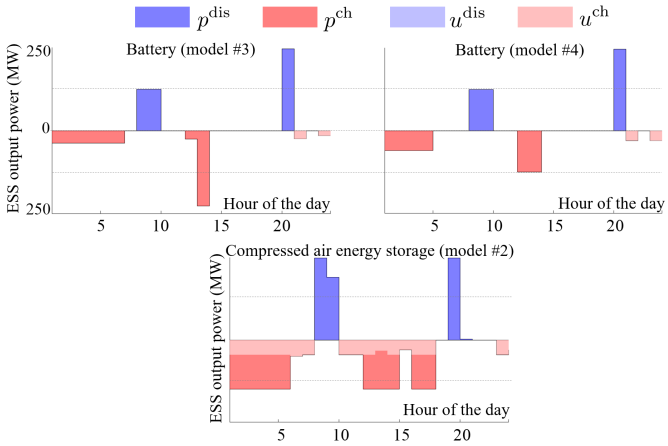

Fig. 12. Day-ahead schedule for the different storage models.

Results reveal that the limited energy storage capacity of batteries prevents them to efficiently participate in the upward reserve market. Indeed, ensuring the real-time availability of the offered capacity would tighten the battery capacity's bounds. In contrast, unit #1 can take advantage of its large energy reservoir to achieve a profit-maximizing inter-temporal and inter-market compromise between offering reserve capacity and energy arbitrage. Unit #2 ($\overline{E}$ = 250 MWh) realizes 70% of its profit via energy arbitrage, while unit #1 ($\overline{E}$ = 1200 MWh) secures 18% of its expected revenues on the energy market. This outcome indicates that energy-constrained technologies may struggle in offering their flexibility directly to the reserve capacity market in the current regulatory framework, which requires a high degree of reliability on delivery.

To compensate its higher operating costs in discharge mode, the CAES system (unit #3) adopts a strategy where most of the upward reserve in provided in charge mode. This results in an asymmetrical participation in the energy market, where the unit charges at intermediate power levels during most periods of the day (to allocate the reserve capacity over the day in level 1, where the probability of activation is the highest), while briefly discharging during peak prices. The strategy thereby decreases the revenues in the energy market to increase those associated with the reserve capacity and balancing markets.

The efficiency of schedules obtained by models #3 and #4 is evaluated in the ex-post analysis using the advanced representation of the battery system. In this way, we observe that disregarding the relation between the state-of-charge and the available charging capacity may lead to an inability to comply with the day-ahead schedule, jeopardizing its operating profit. This is quantified in an ex-post analysis where the simplified model #3 is shown to be unable to follow the (scheduled) high charging power in the early afternoon, resulting in an ex-post profit around 8 % lower than the more realistic model #4, despite a similar expected value (in day-ahead). Furthermore, the storage owner #4 ensures that discharging occurs under a high initial state-of-charge by charging more at the start of the day, and reducing the costs associated with aging effects. Such outcomes clearly illustrate the importance of relying on realistic storage models [40]-[43].

IV. Conclusion

This paper proposes a data-driven methodology to explicitly consider the techno-economic impact of the balancing market outcome into the day-ahead scheduling problem of a strategic ESS owner. This task is challenging due to the inherent difficulty in managing state of charge limitations in the uncertain balancing stage. Firstly, we build a probabilistic model of the time-dependent balancing actions, while differentiating the contributions of reserve providers according to the merit order-based reserve activation. This information is used to ensure probabilistic guarantees on the real-time feasibility of the ESS schedule, with the goal of leveraging more flexibility from storage units. Secondly, we formulate the day-ahead optimization into a tractable single-stage framework that captures the revenues from the day-ahead energy, reserve capacity and real-time balancing markets. The proposed model is generic, hence, one may leverage the formulation of the lower level problem to study the strategic participation of other technologies.

The case study shows that better informing storage owners on the real-time balancing stage allows generating increased profits through more aggressive strategies while maintaining high, user-specified reliability levels. Our results illustrate that storage operators must strive for an accurate probabilistic model of their operating constraints to manage the uncertain balancing market operating conditions rather than relying on a conservative assumption. Additionally, we observe that properly representing the merit order effect is essential to avoid undesired violations of the schedule. An interesting perspective is therefore to integrate uncertainties on the market clearing to fully hedge against strategic behavior of rival technologies, which would be accommodated by the proposed computationally efficient formulation. Also, the proposed framework may serve as a basis to study oligopolistic markets with strategic storage asset owners.

APPENDIX

This appendix contains the more advanced constraints reflecting the actual behavior of a battery storage system (BSS). In particular, we represent two non-linear functions, i.e., $\Delta e_t = f_c(\tilde{e}_t)$ that describes how much energy Δe_t can be charged into the BSS in the next time step, and $\rho_t = f_d(\tilde{e}_t)$ that represents the battery degradation ρ_t. These functions depend on the uncertain real-time state-of-charge $\tilde{e}_t$, which is estimated using the mean activation of the scheduled reserves. To find a compromise between computational burden and modeling accuracy, both non-linear functions are approximated using piecewise linear models.

Practically, the BSS energy content $\tilde{e}_t \in [\underline{E}, \overline{E}]$ is partitioned into $M-1$ subintervals (or segments), corresponding to the following M break points:

$$\underline{E} = E_1 < E_2 < ... < E_M = \overline{E} \tag{A.1}$$

The energy limit of each state of energy segment is then enforced using constraints (A.2)-(A.5), which require introducing $M-1$ binary $z_{t,m}$ and $M-1$ continuous $e_{t,m}$ decision variables at each time step $t \in \mathcal{T}$.

$$z_{t,m} \in \{0,1\}, \;\; \forall t, m = 1, ..., M-1 \tag{A.2}$$

$$\sum_{m=1}^{M-1} z_{t,m} = 1 \;\; \forall t \tag{A.3}$$

$$z_m E_m \leq e_{t,m} \leq z_m \cdot E_{m+1}, \;\; \forall t, m = 1, ..., M-1 \tag{A.4}$$

$$\tilde{e}_t = \sum_{m=1}^{M-1} e_{t,m} \;\; \forall t \tag{A.5}$$

To model the dependence f_c between the charging power limitations and the BSS energy content, we firstly compute the break points of energy charging ability Δe_t, i.e., $C_m = f_c(E_m) \;\; m = 1, ..., M$. This charging potential Δe_t varies thus from C_1 when the BSS is empty, to C_M in case of fully charged battery. Then, the linear approximation can be modeled as follows [43]:

$$\Delta e_t = C_1 + \sum_{m=1}^{M-1} \left(\frac{C_{m+1} - C_m}{E_{m+1} - E_m} e_{t-1,m} \right) \;\; \forall t \tag{A.6}$$

$$p_t^{\text{ch}} \leq \frac{\Delta e_t}{\eta^{\text{ch}}} \;\; \forall t \tag{A.7}$$

The degradation costs C_t^{degr} are integrated into the objective function (2) as an additional (negative) term. In parallel, the following constraint needs to be enforced:

$$C_t^{\text{degr}} \geq C^{\text{B}} \max\{0, (\rho_t - \rho_{t-1})\} \;\; \forall t \tag{A.8}$$

where C^{B} is the battery capital cost (€), and ρ_t is the battery degradation. The degradation break points are given by $D_m = f_d(E_m), \;\; m = 1, ..., M$. The linear interpolation of ρ_t can then be determined as follows:

$$\rho_t = \sum_{m=1}^{M-1} \left(z_{t,m} D_m + \frac{D_{m+1} - D_m}{E_{m+1} - E_m} (e_{t,m} - z_{t,m} E_m) \right) \;\; \forall t \tag{A.9}$$

REFERENCES

[1] J. A. Taylor, D. S. Callaway, and K. Poolla, "Competitive energy storage in the presence of renewables," *IEEE Trans. Power Syst.*, vol. 28, no. 6, pp. 2691–2702, 2013.

[2] Y. Dvorkin, R. Fernandez-Blanco, D. S. Kirschen, H. Pandzic, J. P. Watson, and C. A. Silva-Monroy, "Ensuring Profitability of Energy Storage," *IEEE Trans. Power Syst.*, vol. 32,no. 1, pp. 611–623, 2017.

[3] H. Pandžic, Y. Dvorkin, M. Carrion, "Investments in merchant energy storage: Trading-off between energy and reserve markets," *Appl. Energy*, vol. 230, pp. 277–286, 2018.

[4] P. Zou, Q. Chen, Q. Xia, G. He, and C. Kang "Evaluating the Contribution of Energy Storages to Support Large-Scale Renewable Generation in Joint Energy and Ancillary Service Markets," *IEEE Trans. Sustain. Energy*, vol. 7, no. 2, pp. 808–818, 2016.

[5] J. E. Contreras-Ocaña, M. A. Ortega-Vazquez, and B. Zhang, "Participation of an Energy Storage Aggregator in Electricity Markets," *IEEE Trans. Smart Grid*, vol. 10, no. 2, pp. 1171-1183, March 2019.

[6] S. J. Kazempour, M. Hosseinpour and M. P. Moghaddam, "Self-scheduling of a joint hydro and pumped-storage plants in energy, spinning reserve and regulation markets," *IEEE PES General Meeting*, Calgary, pp. 1-8, 2009.

[7] N. Vespermann, S. Delikaraoglou, and P. Pinson, "Offering Strategy of a Price-Maker Energy Storage System in Day-Ahead and Balancing Markets," *PowerTech IEEE*, Manchester, 2017.

[8] R. Moreno, R. Moreira, and G. Strbac, "A MILP model for optimising multi-service portfolios of distributed energy storage," *Appl. Energy*, vol. 137, pp. 554–566, 2015

[9] G. He, Q. Chen, C. Kang, P. Pinson, and Q. Xia, "Optimal Bidding Strategy of Battery Storage in Power Markets Considering Performance-Based Regulation and Battery Cycle Life," *IEEE Trans. Smart Grid*, vol. 7, no. 5, pp. 2359–2367, 2016.

[10] E. Nasrolahpour, J. Kazempour, H. Zareipour and W. D. Rosehart, "A Bilevel Model for Participation of a Storage System in Energy and Reserve Markets," *IEEE Trans. Sustain. Energy*, vol. 9, no. 2, pp. 582-598, April 2018.

[11] J.-F. Toubeau, Z. De Grève and F. Vallée, "Medium-Term Multimarket Optimization for Virtual Power Plants: A Stochastic-Based Decision Environment," *IEEE Trans. Power Syst.*, vol. 33, no. 2, pp. 1399-1410, March 2018.

[12] H. Akhavan-Hejazi and H. Mohsenian-Rad, "Optimal Operation of Independent Storage Systems in Energy and Reserve Markets With High Wind Penetration," *IEEE Trans. Smart Grid*, vol. 5, no. 2, pp. 1088-1097, March 2014.

[13] H. Ding, P. Pinson, Z. Hu, and Y. Song, "Integrated bidding and operating strategies for wind-storage systems," *IEEE Trans. Sustain. Energy*, vol. 7, no. 1, pp. 163–172, 2016.

[14] M. Kazemi, H. Zareipour, N. Amjady, W. D. Rosehart and M. Ehsan, "Operation Scheduling of Battery Storage Systems in Joint Energy and Ancillary Services Markets," *IEEE Trans. Sustain. Energy*, vol. 8, no. 4, pp. 1726-1735, Oct. 2017.

[15] K. Bruninx, Y. Dvorkin, E. Delarue, D. William, and D. S. Kirschen, "Coupling Pumped Hydro Energy Storage with Unit Commitment," *IEEE Trans. Sustain. Energy*, vol. 7, no. 2, pp. 786–796, 2015.

[16] K. Bruninx, E. Delarue, "Endogenous Probabilistic Reserve Sizing and Allocation in Unit Commitment Models: Cost-Effective, Reliable, and Fast," *IEEE Trans. Power Syst.*, vol. 32, no. 4, pp. 2593–2603, 2017.

[17] A. Schillemans, G. De Vivero Serrano, and K. Bruninx, "Strategic Participation of Merchant Energy Storage in Joint Energy-Reserve and Balancing Markets", *MEDPOWER*, Dubrovnik, 2018.

[18] A. Papavasiliou, S. S. Oren and R. P. O'Neill, "Reserve Requirements for Wind Power Integration: A Scenario-Based Stochastic Programming Framework," *IEEE Trans. Power Syst.*, vol. 26, no. 4, pp. 2197-2206, Nov. 2011.

[19] K. Bruninx and E. Delarue, "Scenario reduction techniques and solution stability for stochastic unit commitment problems," *IEEE International Energy Conference (ENERGYCON)*, Leuven, pp. 1-7, 2016.

[20] European Commission Regulation, "Establishing a guideline on electricity balancing", 2017.

[21] Y. Sun, S. Bahrami, V. W. S. Wong and L. Lampe, "Chance- Constrained Frequency Regulation with Energy Storage Systems in Distribution Networks," *IEEE Trans. Smart Grid*, in press, 2019.

[22] J. Engels, B. Claessens, and G. Deconinck, "Combined stochastic optimization of frequency control and self-consumption with a battery," *IEEE Trans. Smart Grid*, vol. 10, no. 2, pp. 1971–1981, Mar. 2019.

[23] M. Lubin, Y. Dvorkin and S. Backhaus, "A Robust Approach to Chance Constrained Optimal Power Flow With Renewable Generation," *IEEE Trans. Power Syst.*, vol. 31, no. 5, pp. 3840-3849, Sept. 2016.

[24] Y. Guo, K. Baker, E. Dall'Anese, Z. Hu and T. H. Summers, "Data-based distributionally robust stochastic optimal power flow—part I: methodologies," *IEEE Trans. Power Syst.*, vol. 34(2), pp. 1483-1492, March 2019.

[25] H. Zhang, Z. Hu, E. Munsing, S. J. Moura, Y. Song, "Data-Driven Chance-Constrained Regulation Capacity Offering for Distributed Energy Resources," *IEEE Trans. Smart Grid*, vol. 10, no. 3, pp. 2713-2725, 2019.

[26] Y. Ye, D. Papadaskalopoulos, R. Moreira and G. Strbac, "Strategic capacity withholding by energy storage in electricity markets," *PowerTech IEEE*, Manchester, 2017.

[27] E. Nasrolahpour, J. Kazempour, H. Zareipour and W. D. Rosehart, "Impacts of Ramping Inflexibility of Conventional Generators on Strategic Operation of Energy Storage Facilities," *IEEE Trans. on Smart Grid*, vol. 9, no. 2, pp. 1334-1344, March 2018.

[28] Y. Ye, D. Papadaskalopoulos, J. Kazempour and G. Strbac, "Incorporating Non-Convex Operating Characteristics Into Bi-Level Optimization Electricity Market Models," *IEEE Trans. Power Syst.*, vol. 35, no. 1, pp. 163-176, Jan. 2020.

[29] Y. Ye, D. Qiu, M. Sun, D. Papadaskalopoulos and G. Strbac, "Deep Reinforcement Learning for Strategic Bidding in Electricity Markets," *IEEE Trans. on Smart Grid*, vol. 11, no. 2, pp. 1343-1355, March 2020.

[30] R. Chen, I. C. Paschalidis, M. C. Caramanis and P. Andrianesis, "Learning From Past Bids to Participate Strategically in Day-Ahead Electricity Markets," *IEEE Trans. on Smart Grid*, vol. 10, no. 5, pp. 5794-5806, Sept. 2019.

[31] Y. Ye, D. Papadaskalopoulos, R. Moreira, and G. Strbac, "Investigating the impacts of price-taking and price-making energy storage in electricity markets through an equilibrium programming model," *IET Gener., Transmiss. Distrib.*, vol. 13, no. 2, pp. 305–315, Jan. 2018.

[32] A. Shahmohammadi, R. Sioshansi, A.J. Conejo, and S. Afsharnia "Market Equilibria and Interactions Between Strategic Generation, Wind, and Storage." *Appl. Energy*, vol. 220, pp. 876–892, 2018.

[33] M. Dolanyi, K. Bruninx and E. Delarue, "Exposing the Variety of Equilibria in Oligopolistic Electricity Markets," *KU Leuven Energy Systems Integration & Modeling Group Working Paper Series No. ESIM2020-02*, 2019.

[34] M. Hermans, K. Bruninx, K. Van den Bergh, K. Poncelet and E. Delarue, "On the Temporal Granularity of Joint energy-Reserve Markets in a high-RES system," *KU Leuven Energy Institute Working Paper EN2019-13*, 2019.

[35] L. Exizidis, J. Kazempour, P. Pinson, Z. De Grève and F. Vallée, "Impact of Public Aggregate Wind Forecasts on Electricity Market Outcomes," *IEEE Trans. Sustain. Energy*, vol. 8, no. 4, pp. 1394-1405, Oct. 2017

[36] J. Bottieau, L. Hubert, Z. De Grève, F. Vallée and J.-F. Toubeau, "Very-Short-Term Probabilistic Forecasting for a Risk-Aware Participation in the Single Price Imbalance Settlement," *IEEE Trans. Power Syst.*, vol. 35, no. 2, pp. 1218-1230, March 2020.

[37] J.-F. Toubeau, J. Bottieau, F. Vallée and Z. De Grève "Deep Learning-based Multivariate Probabilistic Forecasting for Short-Term Scheduling in Power Markets," *IEEE Trans. Power Syst.*, vol. 34, no. 2, pp. 1203-1215, March 2019.

[38] J.-F. Toubeau, J. Bottieau, F. Vallée and Z. De Grève, "Improved day-ahead predictions of load and renewable generation by optimally exploiting multi-scale dependencies," *IEEE Innovative Smart Grid Technologies - Asia (ISGT-Asia)*, Auckland, pp. 1-5, 2017.

[39] D. Pozo, J. Contreras and E. E. Sauma, "Unit Commitment With Ideal and Generic Energy Storage Units," *IEEE Trans. Power Syst.*, vol. 29, no. 6, pp. 2974-2984, Nov. 2014.

[40] A. Perez, R. Moreno, R. Moreira, M. Orchard and G. Strbac, "Effect of Battery Degradation on Multi-Service Portfolios of Energy Storage," *IEEE Trans. Sustain. Energy*, vol. 7, no. 4, pp. 1718-1729, Oct. 2016.

[41] M. A. Ortega-Vazquez, "Optimal scheduling of electric vehicle charging and vehicle-to-grid services at household level including battery degradation and price uncertainty," *IET Generation, Transmission & Distribution*, vol. 8, no. 6, pp. 1007-1016, Jun. 2014.

[42] A. J. Gonzalez-Castellanos, D. Pozo and A. Bischi, "Non-Ideal Linear Operation Model for Li-Ion Batteries," *IEEE Trans. Power Syst.*, vol. 35, no. 1, pp. 672-682, Jan. 2020.

[43] H. Pandzic and V. Bobanac, "An Accurate Charging Model of Battery Energy Storage," *IEEE Trans. Power Syst.*, vol. 34, no. 2, pp. 1416-1426, March 2019.

[44] Elia Group, "Elia Grid Data," 2019. [Online]. Available: www.elia.be/en/grid-data/data-download.

[45] K. Margellos, P. Goulart and J. Lygeros, "On the Road Between Robust Optimization and the Scenario Approach for Chance Constrained Optimization Problems," *IEEE Trans. Automatic Control*, vol. 59, no. 8, pp. 2258-2263, Aug. 2014.

[46] S. Bolognani, E. Arcari and F. Dörfler, "A Fast Method for Real-Time Chance-Constrained Decision With Application to Power Systems," *IEEE Control Systems Letters*, vol. 1, no. 1, pp. 152-157, July 2017.

[47] G. A. Hanasusanto, V. Roitch, D. Kuhn, and W. Wiesemann, "A distributionally robust perspective on uncertainty quantification and chance constrained programming," *Mathematical Programming*, vol. 151, no. 1, pp. 35-62, 2015.

[48] R. Jiang, and Y. Guan, "Data-driven chance constrained stochastic program," *Mathematical Programming*, vol. 158, no. 1-2, pp. 291-327, 2016.

[49] W. Xie, and S. Ahmed, "On deterministic reformulations of distributionally robust joint chance constrained optimization problems," *SIAM Journal on Optimization*, vol. 28, no. 2, pp. 1151-1182, 2018.

[50] Z. Hu, and L. J. Hong, "Kullback-Leibler divergence constrained distributionally robust optimization," Available at Optimization Online, 2013.

[51] Y. Wang, Y. Dvorkin, R. Fernández-Blanco, B. Xu, T. Qiu and D. S. Kirschen, "Look-Ahead Bidding Strategy for Energy Storage," *IEEE Trans. Sustain. Energy*, vol. 8, no. 3, pp. 1106-1117, July 2017.

[52] Commission for Electricity and Gas Regulation (CREG), "Study on the functioning and price evolution of the Belgian wholesale electricity market monitoring report 2018," 2019.

[53] K. Van den Bergh, D. Couckuyt, E. Delarue, W. D'haeseleer, "Redispatching in an interconnected electricity system with high renewables penetration," *Electr. Pow. Syst. Res.*, vol. 127, pp. 64-72, 2015.

[54] Y. Ye, D. Papadaskalopoulos and G. Strbac, "Investigating the Ability of Demand Shifting to Mitigate Electricity Producers' Market Power," *IEEE Trans. Power Syst.*, vol. 33, no. 4, pp. 3800-3811, July 2018.

[55] K. Bruninx, Y. Dvorkin, E. Delarue, W. D'haeseleer and D. S. Kirschen, "Valuing Demand Response Controllability via Chance Constrained Programming," *IEEE Trans. Sustain. Energy*, vol. 9, no. 1, pp. 178-187, Jan. 2018.

[56] S. A. Gabriel, A. J. Conejo, J. D. Fuller, B. F. Hobbs, and C. Ruiz, *Complementarity Modeling in Energy Markets*, New York, NY, USA: Springer, 2012.

[57] S. Pineda and J. M. Morales, "Solving Linear Bilevel Problems Using Big-Ms: Not All That Glitters Is Gold," *IEEE Trans. Power Syst.*, vol. 34, no. 3, pp. 2469-2471, May 2019.

[58] J.-F. Toubeau, S. Iassinovski, E. Jean, J.-Y. Parfait, J. Bottieau, Z. De Grève, and F. Vallée "Non-linear hybrid approach for the scheduling of merchant underground pumped hydro energy storage," *IET Gener., Transmiss. Distrib.*, vol. 13, no. 21, pp. 4798-4808, 2019.

[59] J.-F. Toubeau, Z. De Grève, P. Goderniaux, F. Vallée and K. Bruninx, "Chance-Constrained Scheduling of Underground Pumped Hydro Energy Storage in Presence of Model Uncertainties," *IEEE Trans. Sustain. Energy*., vol. 11, no. 3, pp. 1516 - 1527, July 2020.

[60] F. Vallée, C. Versèle, J. Lobry, and F. Moiny, "Non-sequential Monte Carlo simulation tool in order to minimize gaseous pollutants emissions in presence of fluctuating wind power," *Renew. Energy*, vol. 50, pp. 317–324, Feb. 2013.

Jean-François Toubeau (M'18) received the degree in civil electrical engineering, and the Ph.D. degree in electrical engineering, from the University of Mons (Belgium) in 2013 and 2018, respectively. He is currently a post-doctoral researcher of the Belgian Fund for Research (F.R.S/FNRS) within the "Power Systems and Markets Research Group" of the same University. He was a visiting researcher at KU Leuven from September 2019 to February 2020. His research mainly focuses on bridging the gap between machine learning and decision-making in modern power systems.

Jérémie Bottieau (S'17) received the Diploma in electrical engineering from he University of Mons, Belgium, where he has been working toward the Ph.D. degree with the "Power Systems and Markets Research Group" since 2017. His research interests include short-term forecasting and optimization in electricity markets.

Zacharie De Grève (M'12) received Electrical and Electronics Engineering degree in 2007 from the Faculty of Engineering of Mons, University of Mons, Belgium, where he received the Ph.D. degree in electrical engineering in 2012. He was a Research Fellow with the Belgian Fund for Research (F.R.S/FNRS) until 2012. He is currently a Researcher with the "Power Systems and Markets Research Group" at the University of Mons, and a part-time Lecturer since September 2019. He conducts transverse research in machine learning, optimization and energy economics, applied to modern electricity networks with a high share of renewables, in order to contribute to the energy transition.

François Vallée (M'09) received the degree in civil electrical engineering and the Ph.D. degree in electrical engineering from the Faculty of Engineering, University of Mons, Belgium, in 2003 and 2009, respectively. He is currently an Associate Professor and leader of the "Power Systems and Markets Research Group" at the University of Mons. His Ph.D. work has been awarded by the SRBE/KBVE Robert Sinave Award in 2010. His research interests include PV and wind generation modeling for electrical system reliability studies in presence of dispersed generation. He is currently a member of the Governing Board from the 'Société Royale Belge des Electriciens - SRBE/KBVE' (2017) and an Associate Editor of the International Transactions on Electrical Energy Systems (Wiley).

Kenneth Bruninx (M'16) received the M.Sc. degree in energy engineering in 2011 and the Ph.D. degree in mechanical engineering in 2016, both from the Univeristy of Leuven (KU Leuven), Belgium. Currently, he is working as a post-doctoral research fellow of the Research Foundation - Flanders (FWO) at (i) the University of Leuven Energy Institute, TME branch (energy conversion), and (ii) EnergyVille.